CLNS 05/1917
CLEO 05-9

Observation of Thirteen New Exclusive Multi-body Hadronic Decays of the $\psi(2S)$

R. A. Briere,[1] G. P. Chen,[1] J. Chen,[1] T. Ferguson,[1] G. Tatishvili,[1] H. Vogel,[1] M. E. Watkins,[1] J. L. Rosner,[2] N. E. Adam,[3] J. P. Alexander,[3] K. Berkelman,[3] D. G. Cassel,[3] V. Crede,[3] J. E. Duboscq,[3] K. M. Ecklund,[3] R. Ehrlich,[3] L. Fields,[3] L. Gibbons,[3] B. Gittelman,[3] R. Gray,[3] S. W. Gray,[3] D. L. Hartill,[3] B. K. Heltsley,[3] D. Hertz,[3] C. D. Jones,[3] J. Kandaswamy,[3] D. L. Kreinick,[3] V. E. Kuznetsov,[3] H. Mahlke-Krüger,[3] T. O. Meyer,[3] P. U. E. Onyisi,[3] J. R. Patterson,[3] D. Peterson,[3] E. A. Phillips,[3] J. Pivarski,[3] D. Riley,[3] A. Ryd,[3] A. J. Sadoff,[3] H. Schwarthoff,[3] X. Shi,[3] M. R. Shepherd,[3] S. Stroiney,[3] W. M. Sun,[3] D. Urner,[3] T. Wilksen,[3] K. M. Weaver,[3] M. Weinberger,[3] S. B. Athar,[4] P. Avery,[4] L. Breva-Newell,[4] R. Patel,[4] V. Potlia,[4] H. Stoeck,[4] J. Yelton,[4] P. Rubin,[5] C. Cawlfield,[6] B. I. Eisenstein,[6] G. D. Gollin,[6] I. Karliner,[6] D. Kim,[6] N. Lowrey,[6] P. Naik,[6] C. Sedlack,[6] M. Selen,[6] E. J. White,[6] J. Williams,[6] J. Wiss,[6] K. W. Edwards,[7] D. Besson,[8] T. K. Pedlar,[9] D. Cronin-Hennessy,[10] K. Y. Gao,[10] D. T. Gong,[10] J. Hietala,[10] Y. Kubota,[10] T. Klein,[10] B. W. Lang,[10] S. Z. Li,[10] R. Poling,[10] A. W. Scott,[10] A. Smith,[10] S. Dobbs,[11] Z. Metreveli,[11] K. K. Seth,[11] A. Tomaradze,[11] P. Zweber,[11] J. Ernst,[12] A. H. Mahmood,[12] H. Severini,[13] D. M. Asner,[14] S. A. Dytman,[14] W. Love,[14] S. Mehrabyan,[14] J. A. Mueller,[14] V. Savinov,[14] Z. Li,[15] A. Lopez,[15] H. Mendez,[15] J. Ramirez,[15] G. S. Huang,[16] D. H. Miller,[16] V. Pavlunin,[16] B. Sanghi,[16] I. P. J. Shipsey,[16] G. S. Adams,[17] M. Cravey,[17] J. P. Cummings,[17] I. Danko,[17] J. Napolitano,[17] Q. He,[18] H. Muramatsu,[18] C. S. Park,[18] W. Park,[18] E. H. Thorndike,[18] T. E. Coan,[19] Y. S. Gao,[19] F. Liu,[19] M. Artuso,[20] C. Boulahouache,[20] S. Blusk,[20] J. Butt,[20] O. Dorjkhaidav,[20] J. Li,[20] N. Menaa,[20] R. Mountain,[20] R. Nandakumar,[20] K. Randrianarivony,[20] R. Redjimi,[20] R. Sia,[20] T. Skwarnicki,[20] S. Stone,[20] J. C. Wang,[20] K. Zhang,[20] S. E. Csorna,[21] G. Bonvicini,[22] D. Cinabro,[22] and M. Dubrovin[22]

(CLEO Collaboration)

[1]*Carnegie Mellon University, Pittsburgh, Pennsylvania 15213*
[2]*Enrico Fermi Institute, University of Chicago, Chicago, Illinois 60637*
[3]*Cornell University, Ithaca, New York 14853*
[4]*University of Florida, Gainesville, Florida 32611*
[5]*George Mason University, Fairfax, Virginia 22030*
[6]*University of Illinois, Urbana-Champaign, Illinois 61801*
[7]*Carleton University, Ottawa, Ontario, Canada K1S 5B6*
and the Institute of Particle Physics, Canada
[8]*University of Kansas, Lawrence, Kansas 66045*
[9]*Luther College, Decorah, Iowa 52101*
[10]*University of Minnesota, Minneapolis, Minnesota 55455*
[11]*Northwestern University, Evanston, Illinois 60208*
[12]*State University of New York at Albany, Albany, New York 12222*
[13]*University of Oklahoma, Norman, Oklahoma 73019*
[14]*University of Pittsburgh, Pittsburgh, Pennsylvania 15260*
[15]*University of Puerto Rico, Mayaguez, Puerto Rico 00681*
[16]*Purdue University, West Lafayette, Indiana 47907*

[17]Rensselaer Polytechnic Institute, Troy, New York 12180
[18]University of Rochester, Rochester, New York 14627
[19]Southern Methodist University, Dallas, Texas 75275
[20]Syracuse University, Syracuse, New York 13244
[21]Vanderbilt University, Nashville, Tennessee 37235
[22]Wayne State University, Detroit, Michigan 48202
(Dated: August 3, 2005)

Abstract

Using data accumulated with the CLEO detector corresponding to an integrated luminosity of $\mathcal{L}$=5.63 pb^{-1} on the peak of the $\psi(2S)$ (3.08×10^6 $\psi(2S)$ decays) and 20.70 pb^{-1} at $\sqrt{s}$=3.67 GeV, we report first measurements of the branching fractions for the following 13 decay modes of the $\psi(2S)$: $\eta 3\pi$, $\eta' 3\pi$, ρK^+K^-, $K^+K^-\pi^+\pi^-\pi^0$, $2(K^+K^-)$, $2(K^+K^-)\pi^0$, $\rho p\bar{p}$, $p\bar{p}\pi^+\pi^-\pi^0$, $\eta p\bar{p}$, $p\bar{p}K^+K^-$, $\Lambda\bar{\Lambda}\pi^+\pi^-$, $\Lambda\bar{p}K^+$, and $\Lambda\bar{p}K^+\pi^+\pi^-$, and more precise measurements of 8 previously measured modes: $2(\pi^+\pi^-)$, $\rho\pi^+\pi^-$, $2(\pi^+\pi^-)\pi^0$, $\omega\pi^+\pi^-$, $K^+K^-\pi^+\pi^-$, ωK^+K^-, ϕK^+K^-, and $p\bar{p}\pi^+\pi^-$. We also report new branching fraction measurements of $\phi\pi^+\pi^-$ and $\omega p\bar{p}$ and upper limits for $\eta\pi^+\pi^-$, ηK^+K^- and $\phi p\bar{p}$. Results are compared, where possible, with the corresponding J/ψ branching ratios to provide new tests of the 12% rule.

The states J/ψ and $\psi(2S)$ are non-relativistic bound states of a charm and an anti-charm quark. In perturbative QCD the decays of these states are expected to be dominated by the annihilation of the constituent $c\bar{c}$ into three gluons or a virtual photon. The partial width for the decays into an exclusive hadronic state h is expected to be proportional to the square of the $c\bar{c}$ wave function overlap at zero quark separation, which is well determined from the leptonic width [1]. Since the strong coupling constant, α_s, is not very different at the J/ψ and $\psi(2S)$ masses, it is expected that for any state h the J/ψ and $\psi(2S)$ branching ratios are related by [2]

$$Q_h = \frac{\mathcal{B}(\psi(2S) \to h)}{\mathcal{B}(J/\psi \to h)} \approx \frac{\mathcal{B}(\psi(2S) \to \ell^+\ell^-)}{\mathcal{B}(J/\psi \to \ell^+\ell^-)} = (12.7 \pm 0.5)\%, \qquad (1)$$

where $\mathcal{B}$ denotes a branching fraction, and the leptonic branching fractions are taken from the Particle Data Group (PDG) [1]. This relation is sometimes called "the 12% rule". Modest deviations from the rule are expected [3]. Although the rule works well for some specific decay modes of the $\psi(2S)$, isospin conserving $\psi(2S)$ decays to two-body final states consisting of one vector and one pseudsoscalar meson exhibit strong suppression: $\rho\pi$ is suppressed by a factor of seventy compared to the expectations of the rule [1, 4–6]. Also, vector-tensor channels such as $\rho a_2(1320)$, and $K^*(892)\bar{K}_2^*(1430)$ are significantly suppressed [1, 7]. A recent review [3] of relevant theory and experiment concludes that current theoretical explanations are unsatisfactory. Clearly, more experimental results are desirable.

This Letter presents new measurements of a wide selection of $\psi(2S)$ decays including modes with and without strange particles and with and without baryons. The following modes of the $\psi(2S)$ are observed for the first time: $\eta 3\pi$, $\eta' 3\pi$, ρK^+K^-, $K^+K^-\pi^+\pi^-\pi^0$, $2(K^+K^-)$, $2(K^+K^-)\pi^0$, $\rho p\bar{p}$, $p\bar{p}\pi^+\pi^-\pi^0$, $\eta p\bar{p}$, $p\bar{p}K^+K^-$, $\Lambda\bar{\Lambda}\pi^+\pi^-$, $\Lambda\bar{p}K^+$, and $\Lambda\bar{p}K^+\pi^+\pi^-$. More precise branching fraction measurements of previously measured modes $2(\pi^+\pi^-)$, $\rho\pi^+\pi^-$, $2(\pi^+\pi^-)\pi^0$, $\omega\pi^+\pi^-$, $K^+K^-\pi^+\pi^-$, ωK^+K^-, ϕK^+K^-, and $p\bar{p}\pi^+\pi^-$ are also reported. We also measure $\phi\pi^+\pi^-$ and $\omega p\bar{p}$ and obtain upper limits for $\eta\pi^+\pi^-$, ηK^+K^- and $\phi p\bar{p}$. Where applicable, the inclusion of charge conjugate modes is implied. As 14 of the modes we study have been previously observed at the J/ψ, 14 tests of the 12% rule are made, 5 for the first time and 9 with greater precision than corresponding previous tests.

The data sample used in this analysis is obtained at the $\psi(2S)$ and the nearby continuum in e^+e^- collisions produced by the Cornell Electron Storage Ring (CESR) and acquired with the CLEO detector. The CLEO III detector [8] features a solid angle coverage for charged and neutral particles of 93%. The charged particle tracking system, operating in a 1.0 T magnetic field along the beam axis, achieves a momentum resolution of $\sim$0.6% at $p = 1$ GeV$/c$. The calorimeter attains a photon energy resolution of 2.2% at $E_\gamma = 1$ GeV and 5% at 100 MeV. Two particle identification systems, one based on energy loss (dE/dx) in the drift chamber and the other a ring-imaging Cherenkov (RICH) detector, are used together to separate $K^\pm$ from $\pi^\pm$. The combined dE/dx-RICH particle identification procedure has efficiencies exceeding 90% and misidentification rates below 5% for both $\pi^\pm$ and $K^\pm$ for the momenta below 2.5 GeV$/c$.

Half of the $\psi(2S)$ data and all the continuum data were taken after a transition to the CLEO-c [9] detector configuration, in which CLEO III's silicon-strip vertex detector was replaced with a six-layer all-stereo drift chamber. The two detector configurations also correspond to different accelerator lattices: the former with a single wiggler magnet and a center-of-mass energy spread of 1.5 MeV, the latter (CESR-c [9]) with six wiggler magnets and an energy spread of 2.3 MeV.

The integrated luminosity ($\mathcal{L}$) of the datasets was measured using e^+e^-, $\gamma\gamma$, and $\mu^+\mu^-$ final states [10]. Event counts were normalized with a Monte Carlo (MC) simulation based on the Babayaga [11] event generator combined with GEANT-based [12] detector modeling. The data consist of $\mathcal{L}$=5.63 pb^{-1} on the peak of the $\psi(2S)$ (2.74 pb^{-1} for CLEO III, 2.89 pb^{-1} for CLEO-c) and 20.70 pb^{-1} at $\sqrt{s}$=3.67 GeV (16 MeV below the $\psi(2S)$, all CLEO-c). The nominal scale factor used to normalize continuum yields to $\psi(2S)$ data is $f_{\rm nom} = 0.270 \pm 0.005$, and is determined from the integrated luminosities of the data sets corrected for the $1/s$ dependence of the cross section, where the error is from the relative luminosity uncertainty, and the uncertainty in the s dependence of the cross section. (The scale factor does not differ appreciably if a high power of $1/s$ is used: a factor of 0.87% for each power). The value of f used for each mode also corrects for the small difference in efficiency between the $\psi(2S)$ and continuum data.

Standard requirements are used to select charged particles reconstructed in the tracking system and photon candidates in the CsI calorimeter. We require tracks of charged particles to have momenta $p > 100$ MeV/c and to satisfy $|\cos\theta| < 0.90$, where θ is the polar angle with respect to the e^+ direction. Each photon candidate satisfies $E_\gamma > 30$ MeV and is more than 8 cm away from the projections of tracks into the calorimeter. Particle identification from dE/dx and the RICH detector is used on all charged particle candidates. Pions, kaons, and protons must be positively and uniquely identified. That is: pion candidates must not satisfy kaon or proton selection criteria, and kaon and proton candidates obey similar requirements. Charged particles must not be identified as electrons using criteria based on momentum, calorimeter energy deposition, and dE/dx.

The invariant mass of the decay products from the following particles must lie within limits determined from MC studies: π^0 ($120 \le M_{\gamma\gamma} \le 150$ MeV), η ($500 \le M_{\gamma\gamma} \le 580$ MeV), η ($530 \le M_{\pi^+\pi^-\pi^0} \le 565$ MeV), ω ($740 \le M_{\pi^+\pi^-\pi^0} \le 820$ MeV [$760 \le M_{\pi^+\pi^-\pi^0} \le 800$ MeV for the $\omega p\bar{p}$ final state]), ϕ ($1.00 \le M_{K^+K^-} \le 1.04$ GeV), and Λ ($1.112 \le M_{p\pi^-} \le 1.120$ GeV). For $\pi^0 \to \gamma\gamma$ and $\eta \to \gamma\gamma$ candidates in events with more than two photons, the combination giving a mass closest to the known π^0 or η mass is chosen, and a kinematically constrained fit to the known parent mass is made. Fake π^0's and η's are suppressed by requiring that each electromagnetic shower profile be consistent with that of a photon. For $\eta \to \pi^+\pi^-\pi^0$ and $\omega \to \pi^+\pi^-\pi^0$, the π^0 is selected as described above, and then combined with all possible combinations of two oppositely charged pions choosing the combination that is closest to the $\eta(\omega)$ mass. A kinematically constrained fit is not used for either of these modes, or for ϕ's or for Λ's. For $\Lambda \to p\pi^-$, a fit of the $p\pi^-$ trajectories to a common vertex separated from the e^+e^- interaction ellipsoid is made. Contamination from K^0_S decays is eliminated by the energy and momentum requirements imposed on the event, and by particle identification.

Energy and momentum conservation requirements are imposed on the reconstructed final state hadrons, which have momentum p_i and combined measured energy $E_{\rm vis}$. We require the measured scaled energy $E_{\rm vis}/E_{\rm c.m.}$ be consistent with unity within experimental resolution, which varies by final state. We require $|\sum \mathbf{p_i}|/E_{\rm c.m.} < 0.02$. Together these requirements suppress backgrounds with missing energy or incorrect mass assignments. The experimental resolutions are smaller than 1% in scaled energy and 2% in scaled momentum.

For the final states with four charged tracks and a π^0, an additional cut is applied to remove a background of radiative events. When the photon is combined with a low-energy photon candidate, it can imitate a π^0. We require $(E_{\rm 4tracks} + E_\gamma)/E_{\rm c.m.} < 0.995$, where E_γ is the energy of the highest energy photon.

In order to compute Q_h in modes with two or more charged pions, two $\pi^{0\prime}$s or an η, it is necessary to remove the contribution from the transitions $\psi(2S) \to J/\psi X$, where $X = \pi^+\pi^-$, $\pi^0\pi^0$, or η [13]. Accordingly we reject events in which the mass of any of the following falls within the range $3.05 < m < 3.15$ GeV [14]: the two highest momentum oppositely charged tracks, the recoil mass against the two lowest momentum oppositely charged tracks, or the mass recoiling against the $2\pi^{0\prime}$s or η.

For every final state, a signal selection range in $E_{\rm vis}/E_{\rm c.m.}$ is determined by Monte Carlo simulation, and a sideband selection range is defined to measure background. Final states with an intermediate ρ, η, η', ω, ϕ or Λ must satisfy a scaled energy signal selection range requirement identical to the corresponding mode without the intermediate particle. For example, the scaled energy signal selection range is the same for ϕK^+K^- and $K^+K^-K^+K^-$. For final states with an η, η', ω, ϕ, or Λ the event yield is determined from signal and sideband selection ranges of the particle mass. For final states with a ρ the event yield is determined from a fit to the $\pi^+\pi^-$ invariant mass by a Breit-Wigner with parameters taken from the PDG [1] (for $\rho\pi^+\pi^-$, the same-sign $\pi^\pm\pi^\pm$ invariant mass distribution is used to estimate the background); an exception is $\rho p\bar{p}$, where the yield is determined from the signal region: $0.54 \leq m_{\pi\pi} \leq 1.0$ GeV assuming a linear background. Most modes studied in this Letter have resonant sub-modes, however; we only report branching ratios for resonant sub-modes which can be cleanly separated from background.

In Fig. 1 the scaled energy and invariant mass distributions are shown for three typical modes: $2(\pi^+\pi^-)$, $2(\pi^+\pi^-)\pi^0$, and $K^+K^-\pi^+\pi^-$. Evidence for production of the ρ, ω and ϕ resonances, respectively, is observed in the corresponding mass spectra.

Event totals are shown for both the $\psi(2S)$ and the continuum in Table I, where $S_{\psi(2S)}$ (S_{co}) is the number of events in the signal region and $B_{\psi(2S)}$ (B_{co}) the number of events in the sideband region in $\psi(2S)$ (continuum) data. Under the assumption that interference between $\psi(2S)$ decay and continuum production of the same final state is absent, the number of events attributable to each $\psi(2S)$ decay mode, N_S, is

$$N_S = S_{\psi(2S)} - B_{\psi(2S)} - f(S_{co} - B_{co}), \tag{2}$$

where f is mode dependent and listed in Table I. We observe a statistically significant signal in all modes except $\eta\pi^+\pi^-$, ηK^+K^- and $\phi p\bar{p}$. The signal with the least statistical significance is $\eta p\bar{p}$ (4.2σ).

The efficiency, ϵ, for each final state is the average obtained from MC simulations [12] for both detector configurations; the two values are typically within a few percent (relative) to each other. No initial state radiation is included in the Monte Carlo, but final state radiation is accounted for. The efficiencies in Table I include the branching ratios for intermediate final states.

We correct N_S by the efficiency and normalize to the number of $\psi(2S)$ decays in the data: 3.08×10^6 determined by the method described in [15]. The resulting branching ratios are listed in Table I, along with a comparison to the PDG [1]. With the exception of $2(\pi^+\pi^-)$ and $\rho\pi^+\pi^-$, none of the branching ratios in [1] were corrected for the contribution from continuum production.

The systematic errors on the ratio of branching fractions share common contributions from the number of $\psi(2S)$ decays (3.0%), uncertainty in f (2.0%), trigger efficiency (1%), and Monte Carlo statistics (2%). Other sources vary by channel. We include the following contributions for detector performance modeling quality: charged particle tracking (0.7% per track), $\pi^0/\eta(\to \gamma\gamma)$ finding (4.4%), Λ finding (3%), $\pi/K/p$ identification

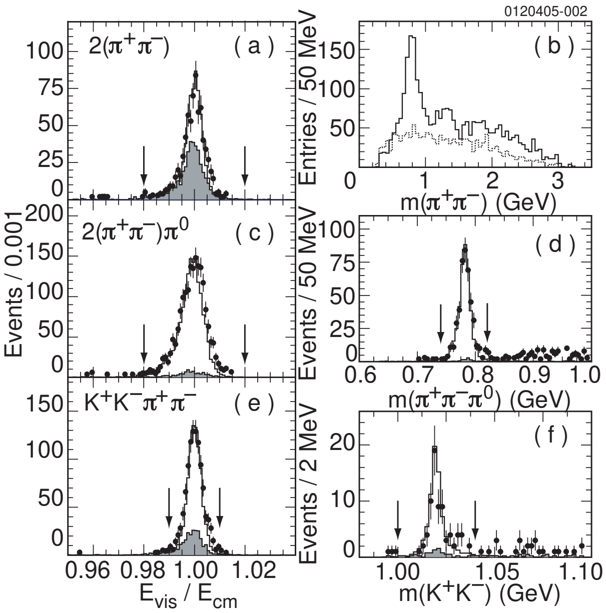

FIG. 1: Distributions for the modes $2(\pi^+\pi^-)$ (a) and (b), $2(\pi^+\pi^-)\pi^0$ (c) and (d), and $K^+K^-\pi^+\pi^-$ (e) and (f). The pairs of arrows indicate the signal regions. (a), (c), and (e) The scaled total energy (filled circle with error bar: $\psi(2S)$ data, solid line: Monte Carlo, shaded histogram: continuum). (b) The $\pi^+\pi^-$ invariant mass in $2(\pi^+\pi^-)$ (solid line: data, dashed line: like sign $\pi^\pm\pi^\pm$ invariant mass, which is used to estimate combinatorial background). (d) The $\pi^+\pi^-\pi^0$ invariant mass in $2(\pi^+\pi^-)\pi^0$(filled circle with error bar: $\psi(2S)$ data, solid line: Monte Carlo, shaded histogram: continuum). (f) The K^+K^- invariant mass in $K^+K^-\pi^+\pi^-$. (The symbol key is the same as (d).)

(0.3%/1.3%/1.3% per identified $\pi/K/p$), and scaled energy and mass resolutions (2%). The systematic error associated with the uncertainty in the level of background is obtained by recomputing the branching ratio when the background at the $\psi(2S)$ and the continuum are coherently increased by 1σ. Since the background in many modes is small, the Poisson probability for the observed number of background events to fluctuate up to the 68% C.L. value is calculated and interpreted as the uncertainty in the level of background. Many of the modes studied have resonant submodes, for example: $2(\pi^+\pi^-)$ where $\rho\pi\pi$ is dominant, $\omega\pi\pi$ where $b_1\pi$ is dominant and $\omega f_2(1270)$ is significant, $K^+K^-\pi^+\pi^-$ where $K^*(892)K\pi$ and ρK^+K^- are large and $\phi\pi^+\pi^-$ is small, and $\eta 3\pi$ where $\eta\pi^0\rho^0$, $\eta\rho^+\pi^-$, and $\eta\rho^-\pi^+$ dominate. The efficiencies for the modes with resonant submodes were weighted using the fractions of the submodes. Allowing for the presence of resonant submodes changes the efficiency by less than 5% relative to the non-resonant efficiency for most modes we have studied. The difference between the weighted efficiency and phase space efficiency is taken as a measure of the uncertainty in the efficiency. For those modes with no observed sub-modes, a conservative 10% uncertainty is assigned for decay model dependence. Systematic uncertainties are significant for all modes and the dominant error for many. The measurements in this Letter are in reasonable agreement with previous measurements where such exist [1].

For the 14 modes where the same final state has been previously measured at the J/ψ, the Q_h value is computed using the absolute $\psi(2S)$ branching ratios determined in this analysis and J/ψ branching ratios from [1] and given in Table I. For 5 of these modes:

TABLE I: For each final state h the following quantities are given: the number of events in the signal region, S_{co}, and background from sidebands, B_{co}, in continuum data; the scale factor, f; the number of events in the signal region, $S_{\psi(2S)}$, and background from sidebands, $B_{\psi(2S)}$, in $\psi(2S)$ data; the number of events attributable to $\psi(2S)$ decay, N_S, computed according to Eq. 2; the average efficiency, ϵ; the absolute branching fraction with statistical (68% C.L.) and systematic errors; previous branching fraction measurements from the PDG [1], and the Q_h value. For $\eta 3\pi$, the two decays modes $\eta 3\pi(\eta \to \gamma\gamma)$ and $\eta 3\pi(\eta \to 3\pi)$ are combined on line $\eta 3\pi$.

mode h	S_{co}	B_{co}	f	$S_{\psi(2S)}$	$B_{\psi(2S)}$	N_S	ε	$\mathcal{B}(\psi(2S) \to h)$ (units of 10^{-4})	$\mathcal{B}$ (PDG) (units of 10^{-4})	Q_h (%)
$2(\pi^+\pi^-)$	1471	28	0.2668	713	20	308.0	0.4507	2.2±0.2±0.2	4.50±1.00	5.55±1.53
$\rho\pi^+\pi^-$	1168	-	0.2667	597	-	285.5	0.4679	2.0±0.2±0.4	4.20±1.50	-
$2(\pi^+\pi^-)\pi^0$	352	25	0.2550	1825	39	1702.6	0.2115	26.1±0.7±3.0	30.00±8.00	7.76±1.10
$\eta\pi^+\pi^-$	15	0	0.2501	13	2	7.2	0.0416	< 1.6	-	-
$\omega\pi^+\pi^-$	43	9	0.2357	437	38	391.0	0.1553	8.2±0.5±0.7	4.80±0.90	11.35±1.94
$\eta 3\pi(\eta \to \gamma\gamma)$	27	2	0.2513	243	35	201.7	0.0639	10.3±0.8±1.4	-	-
$\eta 3\pi(\eta \to 3\pi)$	20	9	0.1820	53	1	50.0	0.0199	8.1±1.4±1.6	-	-
$\eta 3\pi$								9.5±0.7±1.5	-	-
$\eta' 3\pi$	1	0	0.1721	17	4	12.8	0.0092	4.5±1.6±1.3	-	-
$K^+K^-\pi^+\pi^-$	871	83	0.2688	1072	43	817.2	0.3742	7.1±0.3±0.4	16.00±4.00	9.85±3.23
ρK^+K^-	170	-	0.2602	268	-	223.8	0.3361	2.2±0.2±0.4	-	-
$\phi\pi^+\pi^-$	33	13	0.2703	73	20	47.6	0.1744	0.9±0.2±0.1	1.50±0.28	11.07±3.30
$K^+K^-\pi^+\pi^-\pi^0$	634	18	0.2556	888	19	711.6	0.1818	12.7±0.5±1.0	-	10.59±2.81
ηK^+K^-	3	0	0.2396	7	2	4.3	0.0354	< 1.3	-	-
ωK^+K^-	62	12	0.2435	97	8	76.8	0.1288	1.9±0.3±0.3	1.50±0.40	10.19±2.96
$2(K^+K^-)$	100	11	0.2669	85	2	59.2	0.3118	0.6±0.1±0.1	-	6.71±2.74
ϕK^+K^-	46	15	0.2642	49	4	36.8	0.1511	0.8±0.2±0.1	0.60±0.22	5.14±1.53
$2(K^+K^-)\pi^0$	20	0	0.2675	51	1	44.7	0.1339	1.1±0.2±0.2	-	-
$p\bar{p}\pi^+\pi^-$	337	28	0.2509	1010	28	904.5	0.4943	5.9±0.2±0.4	8.00±2.00	9.90±1.16
$\rho p\bar{p}$	23	-	0.2570	67	-	61.1	0.4119	0.5±0.1±0.2	-	-
$p\bar{p}\pi^+\pi^-\pi^0$	204	9	0.2312	499	19	434.9	0.1921	7.3±0.4±0.6	-	18.70±5.80
$\eta p\bar{p}$	2	1	0.2350	12	2	9.8	0.0399	0.8±0.3±0.3	-	3.80±2.09
$\omega p\bar{p}$	26	4	0.2173	37	11	21.2	0.1129	0.6±0.2±0.2	0.80±0.32	4.69±2.22
$p\bar{p}K^+K^-$	25	1	0.2478	37	1	30.1	0.3671	0.3±0.1±0.0	-	-
$\phi p\bar{p}$	2	3	0.2631	6	2	4.3	0.1732	< 0.24	< 0.26	-
$\Lambda\bar{\Lambda}\pi^+\pi^-$	23	4	0.1902	91	14	73.4	0.0844	2.8±0.4±0.5	-	-
$\Lambda\bar{p}K^+$	65	7	0.2586	97	8	74.0	0.2472	1.0±0.1±0.1	-	10.92±2.93
$\Lambda\bar{p}K^+\pi^+\pi^-$	29	3	0.1631	57	7	45.8	0.0847	1.8±0.3±0.3	-	-

$K^+K^-\pi^+\pi^-\pi^0$, $2(K^+K^-)$, $p\bar{p}\pi^+\pi^-\pi^0$, $\eta p\bar{p}$ and $\Lambda\bar{p}K^+$, this is the first measurement of Q_h. All modes except $p\bar{p}\pi^+\pi^-\pi^0$ have Q_h below 12.7%. The modes ϕK^+K^-, $2(\pi^+\pi^-)$, $2(\pi^+\pi^-)\pi^0$, $\eta p\bar{p}$, and $\omega p\bar{p}$ are suppressed with a significance of 4.7, 4.4, 4.1, 4.1, and 3.5 combined statistical and systematic standard deviations, respectively.

In summary we have presented first branching fraction measurements for 13 modes of the $\psi(2S)$: $\eta 3\pi$, $\eta' 3\pi$, ρK^+K^-, $K^+K^-\pi^+\pi^-\pi^0$, $2(K^+K^-)$, $2(K^+K^-)\pi^0$, $\rho p\bar{p}$, $p\bar{p}\pi^+\pi^-\pi^0$, $\eta p\bar{p}$, $p\bar{p}K^+K^-$, $\Lambda\bar{\Lambda}\pi^+\pi^-$, $\Lambda\bar{p}K^+$, $\Lambda\bar{p}K^+\pi^+\pi^-$, and more precise measurements of 8 previously measured modes: $2(\pi^+\pi^-)$, $\rho\pi^+\pi^-$, $2(\pi^+\pi^-)\pi^0$, $\omega\pi^+\pi^-$, $K^+K^-\pi^+\pi^-$, ωK^+K^-, ϕK^+K^-, $p\bar{p}\pi^+\pi^-$. We also measure the branching ratios for $\phi\pi^+\pi^-$ and $\omega p\bar{p}$ and obtain upper limits for $\eta\pi^+\pi^-$, $\eta K^+K^-$and $\phi p\bar{p}$. A full set of measurements of $\pi^+\pi^-+X$, K^+K^-+X and $p\bar{p}+X$ where X is $\rho/\eta/\omega/\phi$ is included in this analysis. Results are compared, where possible, with the corresponding J/ψ branching ratios to test the 12% rule. Five modes are inconsistent with the rule, but all values of Q_h are within a factor of 2 of 12.7%. Since this analysis covers a wide variety of final states including modes with and without strange particles and with and without baryons, the pattern of branching ratios and Q_h values provide tests of theoretical models and should allow new insight into the production widths and the final state interactions operative in the decays of the $\psi(2S)$.

We gratefully acknowledge the effort of the CESR staff in providing us with excellent luminosity and running conditions. This work was supported by the National Science Foundation and the U.S. Department of Energy.

[1] Particle Data Group, S. Eidelman *et al.*, Phys. Lett. B **592**, 1 (2004).

[2] W. S. Hou and A. Soni, Phys. Rev. Lett. **50**, 569 (1983); G. Karl and W. Roberts, Phys. Lett. **144B**, 263 (1984); S. J. Brodsky *et al.*, Phys. Rev. Lett. **59**, 621 (1987); M. Chaichian *et al.*, Nucl. Phys. B **323**, 75 (1989); S. S. Pinsky, Phys. Lett. B **236**, 479 (1990); X. Q. Li *et al.*, Phys. Rev. D **55**, 1421 (1997); S. J. Brodsky and M. Karliner, Phys. Rev. Lett. **78**, 4682 (1997); Y. Q. Chen and E. Braaten, Phys. Rev. Lett. **80**, 5060 (1998); M. Suzuki, Phys. Rev. D **63**, 054021 (2001); J. L. Rosner, Phys. Rev. D **64**, 094002 (2001); J. P. Ma, Phys. Rev. D **65**, 097506 (2002); M. Suzuki, Phys. Rev. D **65**, 097507 (2002).

[3] Y.F. Gu and X.H. Li, Phys. Rev. D **63**, 114019 (2001).

[4] BES Collaboration, M. Ablikim *et al.*, Phys. Lett. B **614**, 37 (2005), Phys. Lett. B **598**, 149 (2004), Phys. Rev. Lett. **93**, 112002 (2004), arXiv:hep-ex/0405030, arXiv:hep-ex/0503040, arXiv:hep-ex/0408047, and Phys. Rev. D **70**, 012003 (2004); BES Collaboration, J.Z. Bai *et al.*, Phys. Rev. D **70**, 012006 (2004).

[5] F. A. Harris, arXiv:hep-ex/0407036 (subm. to Int. J. Mod. Phys. A).

[6] CLEO Collaboration, N.E. Adam *et al.*, Phys. Rev. Lett. **94**, 012005 (2005).

[7] BES Collaboration, J.Z. Bai *et al.*, Phys. Rev. D **69**, 072001 (2004).

[8] CLEO Collaboration, Y. Kubota *et al.*, Nucl. Instrum. Methods Phys. Res., Sect. A **320**, 66 (1992); D. Peterson *et al.*, Nucl. Instrum. Methods Phys. Res., Sect. A **478**, 142 (2002); M. Artuso *et al.*, Nucl. Instrum. Methods Phys. Res., Sect. A **502**, 91 (2003).

[9] CLEO-c/CESR-c Taskforces & CLEO-c Collaboration, Cornell University LEPP Report No. CLNS 01/1742, 2001 (unpublished).

[10] CLEO Collaboration, G. Crawford *et al.*, Nucl. Instrum. Methods Phys. Res., Sect. A **345**, 429 (1994).

[11] C.M. Carloni Calame *et al.*, hep-ph/0312014 *in Proceedings of the Workshop on Hadronic Cross Section at Low Energy (SIGHAD03), 8-10 October 2003, Pisa, Italy,* edited by M. Incagli and G. Graziano (Elsevier, Amsterdam, 2004), p. 258.

[12] Computer code GEANT 3.21, in R. Brun *et al.*, CERN Report No. W5013, (1993) (unpub-

lished).

[13] We do not veto J/ψ from $\psi(2S) \to J/\psi\pi^0$ since it is a very small contribution as $\mathcal{B}(\psi(2S) \to J/\psi\pi^0) = (9.6 \pm 2.1) \times 10^{-4}$ [1].

[14] For the final state $\eta\pi^+\pi^-\pi^0$ we require $2.95 < m < 3.15$ GeV.

[15] CLEO Collaboration, S.B. Athar *et al.*, Phys. Rev. D **70**, 112002 (2004).